Available online at www.sciencedirect.com
ScienceDirect
Journal of Solid State Chemistry 180 (2007) 2143–2148
JOURNAL OF SOLID STATE CHEMISTRY
www.elsevier.com/locate/jssc

Raman-spectroscopic investigation of Ba_2InTaO_6 and Sr_2InTaO_6 perovskites

A. Dias[a,*], L.A. Khalam[b], M.T. Sebastian[b], R.L. Moreira[c]

[a]*Departamento de Química, UFOP, Ouro Preto-MG, 35400-000, Brazil*
[b]*Materials and Minerals Division, Regional Research Laboratory, Trivandrum 695019, India*
[c]*Departamento de Física, UFMG, C.P. 702, Belo Horizonte-MG, 30123-970, Brazil*

Received 19 January 2007; received in revised form 19 May 2007; accepted 24 May 2007
Available online 29 May 2007

Abstract

Raman spectroscopy was employed to investigate the structures and phonon modes of Ba_2InTaO_6 and Sr_2InTaO_6 ceramics. It was found that Ba-based samples belong to the tetragonal $P4/mnc$ (#128 or D_{4h}^6) space group, while Sr-based materials belong to the monoclinic $P2_1/n$ (#14 or C_{2h}^5) space group. Low-temperature measurements did not show any phase transition down to 77 K. Lorentzian lines were used to fit the experimental data, which presented 14 phonon modes for Ba_2InTaO_6 and 24 modes for Sr_2InTaO_6, in perfect agreement with the theoretical factor-group analyses for the proposed structures. This paper reports, for the first time, a tetragonal $P4/mnc$ structure for an indium-containing perovskite material.

Keywords: Perovskites; Indium; Raman spectroscopy; Crystal structures

1. Introduction

Complex double perovskites of the type $A_2B'B''O_6$ have held interest over many years because of their scientific and technological importance [1]. For these ceramics, many chemical substitutions on both *A*- and *B*-sites can be done, which lead to inherent flexibility towards industrial applications [2]. Among these technological demands, the use of double perovskites as dielectric resonators on microwave based wireless communication devices must be emphasized [3]. Recently, indium-containing ceramics have been subject of investigations aiming to determine their structures [4–6]. A_2InBO_6 (A = Ba, Sr and Ca; B = Nb,Ta) materials were first studied in the 1960s by Galasso et al. [7] and Filip'ev et al. [8,9], which observed ordered ceramics but no space group symmetry was given. On the other hand, Yin et al. [10] considered In^{+3} and Nb^{+5} ions randomly distributed and assumed cubic $Pm3m$ symmetry for both Ba_2InNbO_6 and Sr_2InNbO_6 compounds. Ratheesh et al. [11] observed an unresolved Raman spectrum for Sr_2InNbO_6, supporting the random *B*-site ordering, which was also verified for Pb_2InNbO_6 single-crystals by Kania et al. [12].

Ting et al. [4,5] presented a careful structural analysis of A_2InNbO_6 materials by using neutron powder diffraction, electron diffraction and bond valence calculations. In their first report, using a combination of bond valence sum calculations, powder X-ray diffraction and electron diffraction, these authors concluded that Ba_2InNbO_6 occurs in the $Fm\bar{3}m$ elpasolite-type structure, while Sr_2InNbO_6 presents a $P12_1/n1$ ($\equiv P2_1/n$, in a simplified notation) monoclinic perovskite-related superstructure. In their final conclusion, the authors suggested an additional Rietveld refinement through neutron diffraction data in order to enhance the oxygen ions positions. This procedure was conducted and reported by the same authors in a subsequent work [5]. For Sr_2InNbO_6, the monoclinic but "very close to metrically tetragonal" $P2_1/n$ space group symmetry was confirmed, although an additional anti-site refinement indicated that approximately 10% of the In/Nb cations were in "exchanging sites". For Ba_2InNbO_6, the $Fm\bar{3}m$ space group symmetry was found to refine "readily". However, satellite reflections were being

*Corresponding author.
E-mail address: anderson_dias@iceb.ufop.br (A. Dias).

0022-4596/$ - see front matter © 2007 Elsevier Inc. All rights reserved.
doi:10.1016/j.jssc.2007.05.021

systematically over-calculated and attributed to the presence of fine scale translational stacking faults [5]. This evidence comes from the broadening of the satellite reflections as well as from the existence of characteristic anti-phase boundary-type contrast in dark field images. Thus, a "second phase" based on a disordered perovskite parent $P4/mnm$ structure was introduced in order to improve the fitting of the asymmetric parent reflections.

In view of that, it seems that the nice works of Ting et al. [4,5] still leave opened questions, especially for Ba_2InNbO_6 ceramics (where a tetragonal phase was employed to fit the neutron diffraction data). The present paper reports the use of Raman-spectroscopic analysis to investigate the structures of Ba_2InTaO_6 and Sr_2InTaO_6 perovskites. Previous works [13–15] demonstrated the power of this spectroscopic technique to investigate and resolve structures of different complex perovskites based on space group theoretical analysis of their vibrational phonons. Experimental data for both Ta-analog ceramics were obtained from room temperature down to 77 K, in order to determine the correct structure for both materials, and also to investigate structural stability and phonon behavior upon cooling.

2. Experimental

Ba_2InTaO_6 and Sr_2InTaO_6 ceramics were prepared from stoichiometric mixtures of high-purity $SrCO_3$, In_2O_3 and $BaCO_3$ (99.9%; Aldrich Chemical, St. Louis, MO), and Ta_2O_5 (99.9%; Nuclear Fuel Complex, Hyderabad, India) by the solid-state ceramic route. The powders were ball milled for 48 h using zirconia balls in distilled water. The slurry was dried and double calcined at 1375 °C (Ba_2InTaO_6) and 1250 °C (Sr_2InTaO_6), for 4 h. The calcined powders were ground well and mixed thoroughly with 3 wt% polyvinyl alcohol-PVA (BDH Laboratory, Poole, U.K.; molecular weight ≈ 22 000, degree of hydrolysis ⩾98%) solution. Around 0.5 mL of PVA was added to 10 g of the ceramic powder. The slurries were dried and pressed into cylindrical compacts of diameter 14 mm and height 7–9 mm under a pressure of 150 MPa. The green compacts were sintered at 1625 °C (Ba_2InTaO_6) and 1600 °C (Sr_2InTaO_6), for 4 h. The bulk densities of the sintered samples were measured by the Archimedes method. X-ray diffractograms were collected using a modified Rigaku powder apparatus (Geigerflex 2037), equipped with a Cu−Kα source (with graphite monochromator) and automatic data collection.

Micro-Raman scattering spectra were collected using a triple-monochromator Dilor XY spectrometer, equipped with a liquid-N_2-cooled charge-coupled-device detector and an Olympus BXL microscope (100 × objective). The measurements were done in back-scattering geometry using the 514.5 and 647.1 nm lines of an Ar^+ laser (2.5 mW) as exciting source. Low-temperature measurements were carried out in a triple-monochromator Jobin Yvon T64000 spectrometer with an Olympus microscope (20 × objective), from 77 to 300 K in a controlled (Lakeshore) gas flow cryostat (Janis) with an accuracy of about 0.1 K. Measurements were done by using the second harmonic of a YVO_4: Nd laser line as excitation source (532 nm, and effective 10 mW at the sample's surface). Accumulation times were typically 10 collections of 30 s and the spectral resolution was better than 2 cm^{-1}. The resulting spectra were corrected by the Bose–Einstein thermal factor.

3. Results and discussion

First, XRD was employed to investigate the quality of our samples. Fig. 1 presents the results, which showed that single-phase materials were produced without secondary phases or impurities. Also, the profiles of the Ba_2InTaO_6 samples did not present any reflections that could be interpreted as distortions or deviations from cubic symmetry. For Sr_2InTaO_6 ceramics, XRD patterns were indexed by monoclinic structures, as expected. This initial procedure was important to conduct the Raman analysis in well-characterized samples, whose diffractograms are very similar to those obtained by other authors [4,5,16,17]. Thus, according to XRD data, our samples seem to be cubic (Ba) and monoclinic (Sr).

Room temperature Raman analysis was then carried out in both Ba_2InTaO_6 and Sr_2InTaO_6 materials, and the results are displayed in Fig. 2. As it can be seen, two different spectral profiles are clearly observed, which indicates that the ceramics likely occur in different structures. For Ba-based perovskites, dominating bands centered at 100, 390, 550, and 800 cm^{-1} are present, which was previously observed in similar 1:1 ordered ceramics

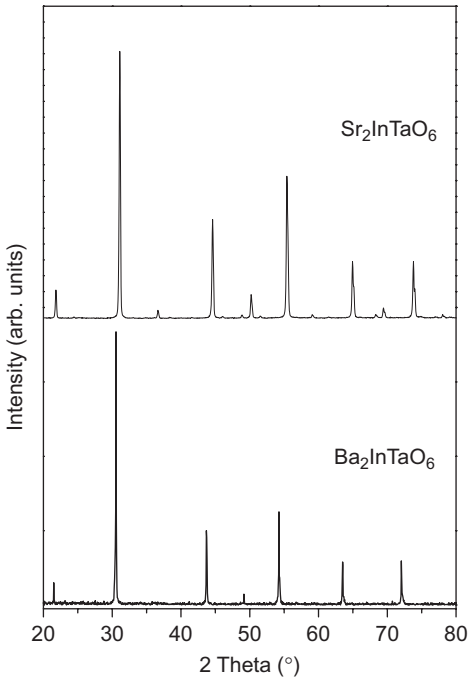

Fig. 1. XRD data for the double perovskites investigated.

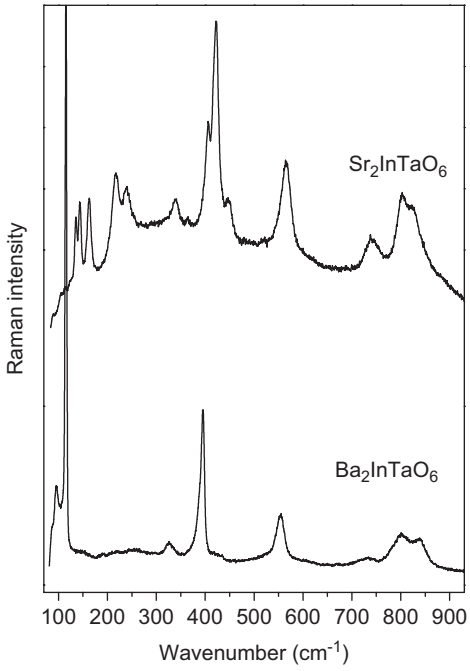

Fig. 2. Room temperature Raman spectra of the Ba_2InTaO_6 and Sr_2InTaO_6 complex perovskites.

[14,18]. Sr-based perovskites showed phonon modes centered in similar positions besides many additional strong bands in the region $150-350\,cm^{-1}$, probably associated with a lower-symmetry structure. As a general trend, the bands of the Sr_2InTaO_6 ceramics are up-shifted compared to their Ba-analogues. This is as a consequence of the smaller Sr ions compared to Ba ions, which leads to a contracted unit-cell, with smaller ionic distances and, then, to general stronger ionic bonds.

For complex cubic perovskites of general formula $A_2B'B''O_6$, a $Fm\bar{3}m$ symmetry is frequently expected in ordered lattice arrangements with 1:1 ratio. This configuration allows a classification of the normal modes at the Brillouin zone-center as:

$$\Gamma = A_g \oplus E_g \oplus F_{1g} \oplus 2F_{2g} \oplus 5F_{1u} \oplus F_{2u}. \quad (1)$$

The resulting factor-group analysis indicates that four modes are Raman-active ($A_g, E_g, 2F_{2g}$), and also four modes are infrared-active ($4\,F_{1u}$) [11]. For the Ba_2InTaO_6 ceramics, XRD data showed that a $Fm\bar{3}m$ structure could be possible, agreeing with most literature available so far. However, an easy inspection of the Raman spectrum (Fig. 2) shows that this material presents a larger number of features than the four dominating Raman-active modes. Then, we take the previous results developed by Ting et al. [4,5] to help us to start a new group theory analysis in a more realistic basis. Assuming the conclusions from Ting et al. [5] for a tetragonal structure, set in space group $P4/mnc$, Ba_2InTaO_6 materials could be described as belonging to the D^6_{4h} space-group. For this structure, the Ba atoms occupy $4d$ sites of special D'_2 symmetry, the In and Ta ions occupy $2a$ and $2b$ sites of C_{4h} symmetry, and the oxygen atoms are in the $8h$ and $4e$ sites (C^h_s and C_4 symmetries, respectively). Then, using the site group method of Rousseau et al. [19] it is possible to obtain the following distribution in terms of the irreducible representations of the D_{4h} point group:

$$\Gamma = 3A_{1g} \oplus 4A_{2g} \oplus 3B_{1g} \oplus 2B_{2g} \oplus 6E_g \oplus 4A_{1u} \oplus 5A_{2u} \oplus 2B_{1u} \oplus B_{2u} \oplus 12E_u. \quad (2)$$

Thus, excluding the silent modes ($4A_{2g}$), we would expect 14 Raman modes ($3A_{1g}, 3B_{1g}, 2B_{2g}, 6E_g$) for this group. Let us now assume the monoclinic $P2_1/n$ space group (C^5_{2h}) for the Sr_2InTaO_6 ceramics, according to the suggestions of Ting et al. [4,5]. In this case, In and Ta ions should occupy the $2a$ and $2b$ Wyckoff-sites of both C_i symmetry, and Sr and O ions would be in $4e$ sites of general C_1 symmetry. The site group method leads now to the following distribution of irreducible representations of the C_{2h} point group:

$$\Gamma = 12A_g \oplus 12B_g \oplus 18A_u \oplus 18B_u. \quad (3)$$

For Sr_2InTaO_6, one would have 24 Raman-active phonon modes ($12A_g, 12B_g$).

Based on the above factor-group analyses, careful fitting of Raman spectra of both Ba_2InTaO_6 and Sr_2InTaO_6 samples were carried out. The results for Ba-based compound are displayed in Fig. 3, which shows the spectrum obtained at 300 K divided in two wavenumber regions, $80-360\,cm^{-1}$ (Fig. 3a) and $360-950\,cm^{-1}$ (Fig. 3b), for better visualization. For this sample, the experimental data are rather scattered, particularly for the first region (Fig. 3a), which sometimes makes it difficult to have the correct fitting of the spectrum. In order to improve the analysis and investigate the structural stability, low-temperature Raman measurements were conducted down to 77 K. Although the results did not bring any improvement in the quality of collected data (inset in Fig. 3b), they show the absence of phase transitions towards lower-symmetry structures. Therefore, the mode depicting was done on the room temperature spectra. The final fitting (black lines in Fig. 3) was obtained through a sum of 14 Lorentzian lines, in good agreement with the theoretical predictions. Table 1 presents the parameters after deconvolution of the spectrum of Ba_2InTaO_6: wavenumbers (cm^{-1}) and full width at half-maxima (cm^{-1}) for the phonon modes identified on the experimental data. Thus, the correct structure for the Ba_2InTaO_6 perovskites appears to be within the tetragonal $P4/mnc$ (D^6_{4h}) space group, which agrees with the assumptions of Ting et al. [5] after neutron diffraction analysis.

Fig. 4 presents the Raman spectra for the Sr_2InTaO_6 perovskite, divided in three spectral regions for better visualization: $50-300\,cm^{-1}$ (Fig. 4a), $300-650\,cm^{-1}$ (Fig. 4b), and $650-950\,cm^{-1}$ (Fig. 4c). Experimental data did not scatter as for Ba_2InTaO_6 materials, which was beneficial for the analysis conducted in the spectrum obtained at 300 K. Low-temperature measurements down to 77 K (inset of Fig. 4b) showed similar results to

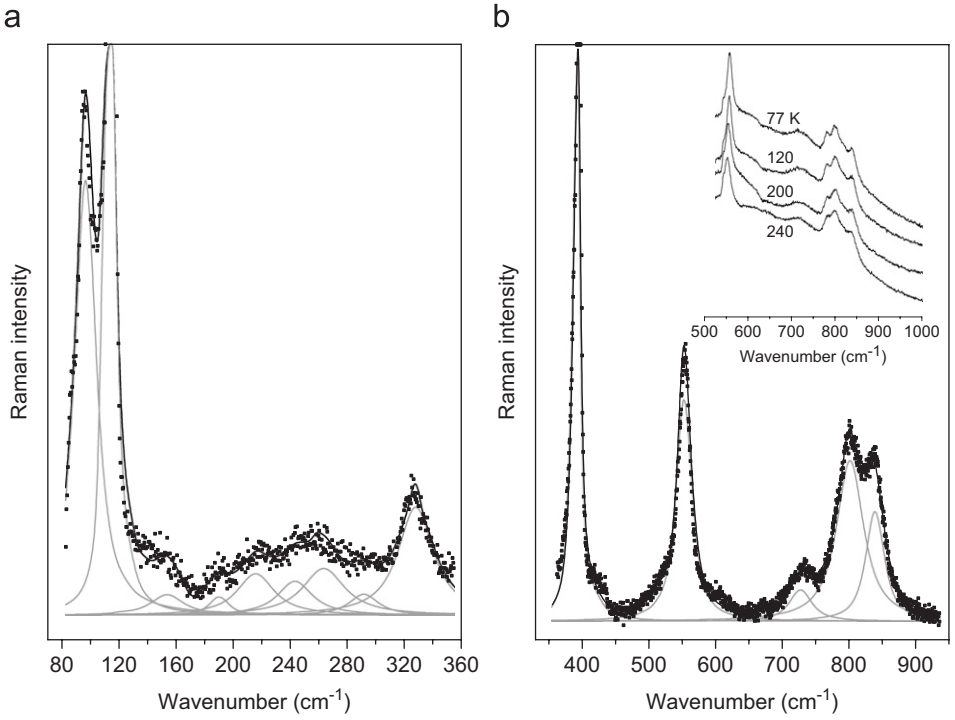

Fig. 3. Raman spectra for Ba_2InTaO_6 ceramics: (a) $80-360\,cm^{-1}$ and (b) $360-950\,cm^{-1}$. Experimental data are in solid squares, while the fitting curve is the black line. Gray lines represent the phonon modes adjusted by Lorentzian curves. Inset in (b): low-temperature spectra.

Table 1
Raman fitting parameters for Ba_2InTaO_6 ceramics

Band	Wavenumber (cm^{-1})	FWHM (cm^{-1})
1	97	16
2	115	3
3	154	26
4	190	14
5	215	30
6	243	28
7	263	34
8	291	23
9	327	28
10	394	11
11	553	23
12	727	36
13	801	45
14	839	28

Ba-based samples, without phase transitions and no improvements towards a higher resolution (particularly, peak splitting were not observed). Because of increasing luminescence effects for decreasing temperatures, fitting was conducted in the spectrum obtained at 300 K and 24 Lorentzian lines could be depicted, in perfect agreement with the hypothesis for a monoclinic $P2_1/n$ (C_{2h}^5) structure. Table 2 presents the parameters after deconvolution of the spectrum of Sr_2InTaO_6 for the phonon modes identified on the experimental data. Sr-based complex perovskites are frequently found to belong to lower-symmetry structures (as well as Ca-based materials) due to the smaller Sr ions compared with the analogous Ba perovskites, which lead to distorted (tilted) structures [4–6].

Howard et al. [20] have used group-theoretical methods to enumerate the structures of ordered double perovskites by considering different combinations of octahedral tilting. This tilting is usually driven by a mismatch in the size of the *A*-site cation and the size of the cubo-octahedral cavity. Ideal cubic simple perovskites belong to the space group $Pm\bar{3}m$, while doubling of the ideal perovskite by imposition of rock-salt 1:1 ordering leads to cubic $Fm\bar{3}m$ structure. For this structure, tiltings of the BO_6 octahedra are allowed and hence lower-symmetry structures would result. Howard et al. [20] found 11 lower-symmetry structures derived from the $Fm\bar{3}m$ cubic space group as a result of the cation ordering in combination with the corner-linked tilting of the octahedral units. Group–subgroup relationships were established and help us to explain the experimentally observed structures in Ba_2InTaO_6 and Sr_2InTaO_6 perovskites studied in the present work, as discussed below.

Ba_2InTaO_6 perovskites present tolerance factor ≈ 1.009 [16,17], which means that a cubic structure is expected. Many other complex perovskites with tolerance factors near to the unity (or traditionally considered cubic) were recently revisited and distorted structures were determined [14]. For Ba_2YNbO_6, Dias et al. [14] showed that although XRD and other techniques indicate cubic or nearly cubic structures, Raman-spectroscopic analysis demonstrated a tetragonal $I4/m$ structure for these materials. According to the Glazer notation [21], the $I4/m$ structure derives from

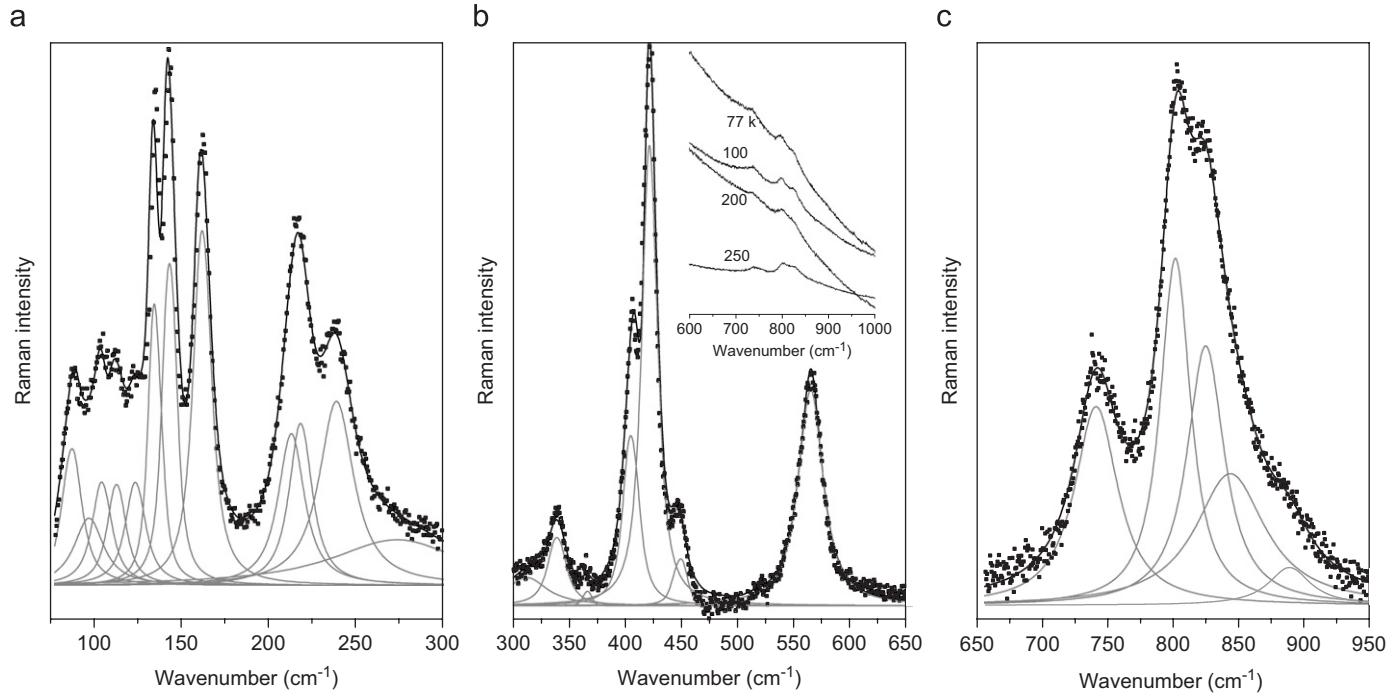

Fig. 4. Raman spectra for Sr_2InTaO_6 ceramics: (a) $50-300\,cm^{-1}$; (b) $300-650\,cm^{-1}$; and (c) $650-950\,cm^{-1}$. Experimental data are in solid squares, while the fitting curve is the black line. Gray lines represent the phonon modes adjusted by Lorentzian curves. Inset in (b): low-temperature spectra.

Table 2
Raman fitting parameters for Sr_2InTaO_6 samples

Band	Wavenumber (cm^{-1})	FWHM (cm^{-1})
1	88	12
2	98	19
3	105	12
4	113	11
5	124	12
6	135	6
7	144	7
8	162	10
9	213	17
10	219	14
11	239	23
12	274	71
13	312	42
14	339	16
15	364	4
16	405	13
17	422	13
18	449	9
19	565	24
20	741	39
21	802	26
22	825	33
23	844	64
24	889	37

the $Fm\bar{3}m$ ($a^0a^0a^0$) by a single rotation of the BO_6 octahedra about one of the fourfold axes, lowering the symmetry to tetragonal ($a^0a^0c^-$). This structure presents 9 Raman-active bands [14], which is not compatible with our findings for the Ba_2InTaO_6 perovskite. We believe that the small tetragonal distortion in this material is similar to that observed in Ba_2YNbO_6, i.e., the octahedral tilting is too small to be detected by XRD or even more sophisticated techniques, like neutrons and electron diffraction. However, the out-of-phase distortions appear to be sufficiently large to be detected by Raman spectroscopy.

We start with the same hypothesis for a distorted structure by tilting only one axis (smaller possible distortion), and using group–subgroup relationships developed by Howard et al. [20]. From the $Fm\bar{3}m$ space group, there are only two possibilities: $I4/m$ ($a^0a^0c^-$), discussed above, and $P4/mnc$ ($a^0a^0c^+$). The only difference between them is the direction of the distortion: out-of-phase for the former and in-phase for the last space group. Both structures are tetragonal and the $P4/mnc$ space group applied to our Ba_2InTaO_6 materials agrees well with the number of Raman-active modes experimentally verified. Also, fortunately, this structure represents the intermediate phase between the $Fm\bar{3}m$ cubic and the monoclinic $P2_1/n$ ($a^+b^-b^-$), assumed in the present work as being the correct structure for Sr_2InTaO_6 perovskites. In this respect, Howard et al. [20] pointed out this phase transformation as a continuous $Fm\bar{3}m \rightarrow P4/mnc \rightarrow P2_1/n$ "natural" sequence. The authors appeared to be surprised for the fact that "there has been no report to date of the direct observation of the intermediate tetragonal structure in $P4/mnc$ space group". In this respect, experimental Raman data allowed us to determine the correct structure for Ba_2InTaO_6 and Sr_2InTaO_6 perovskites at the light of

group-theoretical models. Besides, these results contributed to understand and explain small distortions in materials with tolerance factors close to the unity (considered ideally cubic), and to report the first example of a $P4/mnc$ indium-containing tetragonal perovskite.

4. Conclusions

The crystal structures of Ba_2InTaO_6 and Sr_2InTaO_6 perovskites were analyzed by Raman spectroscopy, from room temperature down to 77 K. Based on XRD data and on the available literature, we have investigated the possibilities for a non-cubic structure for Ba_2InTaO_6 and discussed the expected results for the monoclinic structure proposed for the Sr-based analog perovskite. The results showed quite different spectra for the analyzed materials, which in turn are similar for each perovskite for decreasing temperatures. No phase transition was detected for both ceramics down to 77 K. Room temperature spectra were fitted by sum of Lorentzian lines, and a tetragonal $P4/mnc$ (D^6_{4h}) structure (14 Raman-active phonon modes) was found for Ba_2InTaO_6. On the other hand, Sr-based materials belong to the monoclinic $P2_1/n$ (C^5_{2h}) space group, with 24 Raman bands clearly identified. In both cases, the results are in perfect agreement with the theoretical factor-group analysis for the assumed structures. This paper reports for the first time a tetragonal $P4/mnc$ structure for a indium-containing perovskite material.

Acknowledgments

The Brazilian authors acknowledge the financial support from MCT/CNPq, FINEP and FAPEMIG. Indian authors are grateful to CSIR. One of the authors (L.A. Khalam) thanks UGC for the award of a fellowship. Special thanks to Prof. F.M. Matinaga (UFMG) for his hospitality during low-temperature Raman experiments.

References

[1] T.A. Vanderah, Science 298 (2002) 1182–1184.
[2] W. Wersing, Curr. Opin. Solid State Mater. Sci. 1 (1996) 715–731.
[3] I.M. Reaney, D.M. Iddles, J. Am. Ceram. Soc. 89 (2006) 2063–2072.
[4] V. Ting, Y. Liu, R.L. Withers, E. Krausz, J. Solid State Chem. 177 (2004) 979–986.
[5] V. Ting, Y. Liu, R.L. Withers, L. Norén, M. James, J.D. Fitz Gerald, J. Solid State Chem. 179 (2006) 551–562.
[6] W.T. Fu, D.J.W. Ijdo, Solid State Commun. 134 (2005) 177–181.
[7] F. Galasso, W. Darby, J. Phys. Chem. 66 (1962) 131–132.
[8] V.S. Filip'ev, E.G. Fesenko, Sov. Phys.-Crystallogr. 10 (1966) 243–247.
[9] V.S. Filip'ev, E.G. Fesenko, Sov. Phys.-Crystallogr. 10 (1966) 532–534.
[10] J. Yin, Z. Zou, J. Ye, J. Phys. Chem. B 107 (2003) 61–65.
[11] R. Ratheesh, M. Wöhlecke, B. Berge, Th. Wahlbrink, H. Haeuseler, E. Rühl, R. Blachnik, P. Balan, N. Santha, M.T. Sebastian, J. Appl. Phys. 88 (2000) 2813–2818.
[12] A. Kania, K. Roleder, G.E. Kugel, M. Hafid, Ferroelectrics 135 (1992) 75–84.
[13] R.L. Moreira, F.M. Matinaga, A. Dias, Appl. Phys. Lett. 78 (2001) 428–430.
[14] A. Dias, L.A. Khalam, M.T. Sebastian, C.W.A. Paschoal, R.L. Moreira, Chem. Mater. 18 (2006) 214–220.
[15] R.L. Moreira, A. Feteira, A. Dias, J. Phys.: Condens. Matter 17 (2005) 2775–2781.
[16] L.A. Khalam, H. Sreemoolanathan, R. Ratheesh, P. Mohanan, M.T. Sebastian, Mater. Sci. Eng. B 107 (2004) 264–270.
[17] L.A. Khalam, M.T. Sebastian, Int. J. Appl. Ceram. Technol. 3 (2006) 364–374.
[18] R.L. Moreira, L.A. Khalam, M.T. Sebastian, A. Dias, J. Eur. Ceram. Soc. 27 (2007) 2803–2809.
[19] D.L. Rousseau, R.P. Bauman, S.P.S. Porto, J. Raman Spectrosc. 10 (1981) 253–290.
[20] C.J. Howard, B.J. Kennedy, P.M. Woodward, Acta Cryst. B59 (2003) 463–471.
[21] A.M. Glazer, Acta Cryst. A 31 (1975) 756–762.